Uncertainty and Sensitivity Analysis in Complex Plasma Chemistry Models

Miles M. Turner

School of Physical Sciences and National Centre for Plasma Science and Technology, Dublin City University, Dublin 9, Ireland

E-mail: miles.turner@dcu.ie

Abstract. The purpose of a plasma chemistry model is prediction of chemical species densities, including understanding the mechanisms by which such species are formed. These aims are compromised by an uncertain knowledge of the rate constants included in the model, which directly causes uncertainty in the model predictions. We recently showed that this predictive uncertainty can be large—a factor of ten or more in some cases. There is probably no context in which a plasma chemistry model might be used where the existence of uncertainty on this scale could not be a matter of concern. A question that at once follows is: Which rate constants cause such uncertainty? In the present paper we show how this question can be answered by applying a systematic screening procedure—the so-called Morris method—to identify sensitive rate constants. We investigate the topical example of the helium-oxygen chemistry. Beginning with a model with almost four hundred reactions, and focussing on conditions relevant to biomedical applications, we show that only about fifty rate constants materially affect the model results, and as few as ten cause most of the uncertainty. This means that the model can be improved, and the uncertainty substantially reduced, by focussing attention on this tractably small set of critical rate constants. We discuss strategies that might be used to accomplish this refinement. The present results apply to a particular chemistry, but we suggest that possibly, and perhaps probably, investigations of other plasma chemistry models will arrive at similar results. In that case, an opportunity exists to systematically improve the quality of plasma chemistry modelling.

PACS numbers:

1. Introduction

Modelling work directed at understanding or optimizing low-temperature plasma processes usually incorporates a plasma chemistry model. Such models can be complex. For instance, recent work on air chemistry has involved models with many hundreds of rate constants and several tens of plasma species [40, 14, 36]. These models tend towards maximal complexity, in the sense that they incorporate every chemical process and reaction pathway that could reasonably be thought relevant. The rationale for this approach is, presumably, that a larger model is likely to give "better" predictions, for example because an important reaction pathway is less likely to be omitted in error. This philosophy has apparently informed the development of chemistry models in the low-temperature plasma physics community for the last few decades, which have seen the complexity of models steadily increasing. However, other communities facing similar difficulties, such as combustion science, have tended towards a different approach [51, 41, 44, 23, 35]. They favour smaller models, with perhaps a few tens of chemical processes. The advantage of this method is that critical attention is focussed on a rather small set of processes that have been identified as important. Of course, this reduction in model complexity is gained in part by limiting the scope of the model, for instance by restricting the parameter space of applicability, or reducing the number of species whose density is to be predicted.

There is another consideration. None of these models is capable of precise prediction, because the rate constants that they include are not exactly known. This uncertainty in model parameters causes uncertainty in model predictions. In low-temperature plasma physics, at least, this uncertainty has rarely been quantified, and is usually ignored, but is always present. Clearly, the inclusion in a model of reactions whose influence on the model results is appreciably less than the margin of parametric uncertainty cannot be regarded as an improvement, and may have adverse consequences. These might include dilution of the resources available for researching rate data, obfuscation of the important reaction pathways, and wasteful use of computer resources, especially if the model is intended as an element in a larger construct, such as a multi-dimensional simulation.

These arguments suggest that, in the context of low-temperature plasma physics, a reduction in the complexity of chemistry models may be desirable, and may be delivered without compromising the predictive power of models. A criterion for judging whether this has been achieved is that the predictions of the simplified models should remain within the parametric uncertainty envelope established for a related comprehensive model. As this presumably cannot be shown for every conceivable condition, this approach entails that some zone of applicability for the simplified model is specified *a priori*.

In the present paper, we investigate the application of these strategies to a particular plasma chemistry, namely mixtures of helium and oxygen. This has topical interest, because of emerging biomedical applications [15]. In a previous paper [49], we discussed a

comprehensive model for this chemistry, and we investigated the parametric uncertainty in the model predictions associated with the uncertainty in the rate constants employed. This comprehensive model includes some twenty five chemical species, and about three hundred and seventy chemical processes. The parametric uncertainty in the model predictions strongly depends on the chemical species and the particular plasma conditions, but is rarely less than ten percent and may exceed a factor of ten. We will show below that if we limit our ambition to predicting the densities of species likely to be of biological interest, under operating conditions relevant to biological applications, then the number of species in the model can be reduced from twenty five to twelve, and the number of reactions from three hundred and seventy to about fifty, under the criterion suggested above, that the model predictions have not changed, within the margin of parametric uncertainty.

We then proceed to a global sensitivity analysis, which associates the uncertainty in the model predictions with particular rate constants. This exercise shows that only about ten rate constants ever contribute more than ten percent to the uncertainty in any chemical species density. This suggests that efforts to improve the quality of prediction using this model can focus narrowly on this set of influential rate constants. Moreover, one can often identify regions of parameter space where some species density is highly sensitive to a particular rate constant. There are, therefore, opportunities for validating experiments to focus on these sensitive regions, and hence refine the most influential rate constants. Thus one can envisage a validation strategy that would systematically improve the model, by reducing the parametric uncertainty. One could also use this sensitivity data to motivate independent experiments to refine particular rate constants. However, in practice, the rate constants most in need of refinement prove to be those that have, for various reasons, previously proved resistant to precise experimental determination.

In the next section, we describe the procedure that was used to identify reactions that are of little importance under the conditions of interest, and hence we develop a model with a reduced set of reactions. Then, in section 3, we apply a screening procedure to select those reactions whose rate constants appreciably influence the uncertainty in the model predictions. The significance of the results of this process is discussed in section 4, before we proceed to conlude in section 5.

2. Model Reduction

As noted above, an aim of the present work is to develop a model for helium-oxygen plasma chemistry that excludes unimportant reactions, where "unimportant" is to be judged by reference to the parametric uncertainty that necessarily affects the model predictions, because of the uncertainty in the rate constants incorporated in the model, as the introduction explains. We limit our consideration to operating conditions that are typical for atmospheric pressure plasma sources designed for biomedical applications, such as the so-called micro-atmospheric pressure plasma jet (μAPPJ) [43]. In this

source, the feedstock gas flows through a channel with dimensions of approximately $1 \times 1 \times 30$ mm^{-3}. A pair of plane electrodes form opposing sides of the channel, while the remaining sides are quartz plates, which both confine the discharge and provide access to optical diagnostics. The feedstock gas consists of a trace of oxygen (up to a few percent) in a buffer of helium. Under typical operating conditions, the gas residence time in the channel is a few milliseconds. The operating power is constrained both by discharge stability considerations and the desire to prevent significant gas heating. These factors limit the discharge power to a fraction of a watt. (Much higher powers have sometimes been reported, but these data almost certainly do not properly reflect the power coupled to the plasma.) Our aim is therefore to develop a chemistry model which is applicable to these conditions, which are likely to be representative for the many other sources that are in use, for instance because the gas heating constraint is essentially universal for the intended applications. We note also that not all of the plasma species are of equal interest. In practice, only a few relatively long-lived neutral species reach high densities, and probably only these species are involved in biological interactions. The usual assumption is that in a helium-oxygen chemistry, only atomic oxygen, ozone, and the metastable $O_2(a^1\Delta_u)$ state of the oxygen molecule are in this category [15]. Therefore, our aim is to develop a chemistry model that predicts these species densities consistently with the previous comprehensive model, taking into account the parametric uncertainty in both models. Of course, an implicit feature of this procedure is that we must also adequately predict certain other parameters that are antecedent to these neutral species densities, such as the electron density and temperature.

For the purposes of this work, and as before [49], we use a zero-dimensional representation of the discharge, in which we apply a given power during the nominal residence time of 3 ms, and then follow the evolution of the plasma in the afterglow for a further 3 ms, for a total integration time of 6 ms. In the usual way, we solve balance equations for the species densities and the electron temperature. We assume that the electron energy distribution is Maxwellian, and that the gas temperature is 300 K. Probably neither of these assumptions should ever be made in the context of predicting experimental results [32, 33], but they are adequate for the aims of the present work. We investigated powers between 0.1 and 10 W, and gas mixtures such that $0.05\ \% \leq [O_2]/[He] \leq 3\ \%$. The model reduction was effected through the following steps:

(i) We solved the comprehensive model at a set of operating points spanning the space of interest. Then we analysed the results of these calculations, and discarded all those reactions that never contributed more than 5 % (instantaneously) to the time derivative of any species. Of course, the time integrated contribution of such reactions is likely to be considerably less.

(ii) The $O(^1S)$ atomic oxygen state never reaches a high density, and plays no discernibly important role in the chemistry. This state was therefore eliminated.

(iii) We noted that the presence of vibrationally excited states has no significant effect

under the conditions of interest, and so we removed these states from the model, together with the reactions associated with them.

(iv) The comprehensive model includes a number of complexes of closely linked states, such the helium atomic and molecular metastables, the corresponding ions, and the several positive and negative ions of oxygen. The distribution of these species within the complexes varies with the conditions, under the influence of a large number of reactions, but the overall effect of these changes on the neutral species densities of interest is slight. We therefore replaced these complexes with composite states, so that the reduced model has a single helium excited state, a single helium ion state, and one oxygen ion species of each sign. These then become portmanteau states, and consequently their densities cannot be directly compared with the same species densities in the comprehensive model. For example, the species named "O^-" in the reduced model aggregates O_2^-, O_3^-, and O_4^- in the comprehensive model.

(v) The set of electron impact processes was simplified by reducing the large set of discrete vibrational excitation processes to two processes, representing resonant and non-resonant mechanisms, such that energy loss is preserved. Similarly, distinct excitation processes with the same products and similar thresholds were amalgamated.

These methods lead to the reaction scheme shown in tables 1 and 2. The rate constants are assumed to be expressed in the extended Arhenius form:

$$k(T) = AT^B \exp\left(-\frac{C}{T}\right), \tag{1}$$

where T is either the gas temperature or the electron temperature, and A, B and C are coefficients peculiar to each reaction. Also included in the table is an estimate of the uncertainty in the rate constant, derived from primary sources using principles previously discussed [49]. The uncertainty is assumed to affect only the parameter A. The scheme shown in these tables has 12 plasma species and 51 reactions, compared to 25 species and 373 reactions in the comprehensive model. The number of reactions has thus been reduced by about 85 %. Moreover, the reactions that have been discarded include a disproportionate number based on weak authority. We earlier introduced a classification scheme [49], in which reactions were assigned to one of three categories. In short, category A reactions have some definite authority, category B reactions are derived from some theoretical or semi-empirical procedure, and category C reactions are chosen by analogy with a similar process in category A. Category A reactions thus represent data of the highest quality (although there is considerable variation within this category). In the comprehensive model, about 45 % of the reactions are in category A. In the reduced model, on the other hand, more than 90 % of reactions are in this category. This does not mean, of course, that the reduced model is likely to yield more accurate predictions, because the reactions that have been discarded were not appreciably influencing the results, but it does show that the model is much more solidly

based that first appears. This important observation is obscured by the inclusion in the comprehensive model so many weakly documented processes of minor importance.

In figures 1 to 5 we present a selection of results comparing the comprehensive model with the reduced model developed in the present paper. These results are obtained using the procedure explained in earlier work [49]. In brief, the rate constants are described using probability distributions (in this case, lognormal functions) characterized by the uncertainty parameters shown in table 2. The model is solved many times to generate a population of predictions, each using a different random realisation of the rate constants. This procedure leads to a distribution of predictions, which are characterized by their upper and lower quartile values. The range between these values is indicated by the error bars in the figures. In this way, the uncertainty in the rate constants is mapped to uncertainty in the predicted species densities. Figures 1 and 3 compare the electron densities, as a function of oxygen content and as a function of power. As we remarked above, predicting the electron density is not an explicit objective of the model, but it would be remarkable if the explicit objectives of the model could be achieved without predicting this parameter correctly. So the good agreement seen here is expected. In the remaining figures, we compare the atomic oxygen density at the end of the discharge pulse, as a function of oxygen content, in figure 2, and as a function of power, in figure 4. Finally, we show the atomic oxygen density as a function of oxygen context at the end of the afterglow period, in figure 5. Similarly good agreement is obtained for $O_2(a^1\Delta_u)$ and ozone under the same conditions. These data show that the reduced model is practically indistinguishable from the comprehensive model, under the conditions where the former is designed to be valid. We note, however, that the informal reduction procedure employed here could fail in general. For instance, in the case where a manifold of states are coupled by rapid reactions, but entrance to and exit from the manifold are governed by much slower processes. More formal approaches to chemical model reduction are known, and might prove more robust [28].

The procedure described above yields a simpler model that agrees in every relevant respect with the original comprehensive model. This approach does nothing to reduce the parametric uncertainty in the model predictions, however, nor does it associate the uncertainty with any particular rate constant. In the next section, we apply a screening procedure that aims to identify those rate constants that are primarily responsible for the parametric uncertainty in the model predictions.

3. Sensitivity Analysis

3.1. Screening Procedure

Models containing a large number of uncertain parameters are commonly encountered, and consequently the problem of ranking the parameters in such models has been much discussed [34, 11]. "Ranking" in this context means identifying those parameters that most strongly influence the model predictions. The ranking scheme adopted in the

present work was suggested by Morris [34]. Formally, the problem is to investigate the effect of a vector of "factors" on a vector of "model outputs." In the present study, the factors are the uncertain rate constants, and the model outputs are the species densities. The Morris method assumes that the vector of factors is confined to the unit hypercube, so that each factor takes a value between zero and one, and the number of dimensions of the hypercube is equal to the number of factors. Of course, these values are generally mapped to some less uniform distribution in order to evalate the model. For the purposes of the analysis, each factor is restricted to a finite number of values, so that there is a correspondingly finite number of permitted choices for the vector of factors, which we denote as $\mathbf{X}$. This is equivalent to constructing a lattice that fills the hypercube, such that each vector $\mathbf{X}$ denotes a node of the lattice. The analysis proceeds by investigating so-called "elementary effects." An elementary effect is produced by changing the value of a single factor, and evaluating the effect on the model outputs. Changing a single factor in this way amounts to moving from one node of the lattice to another in a direction parallel to one of the axes. So if the outputs of the model are calculated as $\mathbf{Y}(\mathbf{X})$, then an elementary effect is evaluated as:

$$\Delta\mathbf{Y}_i = \frac{\mathbf{Y}(\mathbf{X} + \Delta\hat{\mathbf{e}}_i) - \mathbf{Y}(\mathbf{X})}{\Delta}, \tag{2}$$

where $\hat{\mathbf{e}}_i$ is a unit vector along the axis corresponding to the ith factor, and Δ is some scalar constant. Of course, we must ensure that the evaluation points remain within the unit hypercube. The Morris method examines a sample of such elementary effects, and then evaluates

$$\mu_{i,j} = \langle \Delta Y_{i,j} \rangle \tag{3}$$

$$\sigma_{i,j} = \sqrt{\left\langle (\Delta Y_{i,j} - \mu_{i,j})^2 \right\rangle}, \tag{4}$$

so that the metrics $\mu_{i,j}$ and $\sigma_{i,j}$ characterise the effect of the ith factor on the jth output. For each output, the magnitude of μ is used to rank the influence of each factor on that output. An alternative metric is μ^*, which is the mean of the absolute values of ΔY. This avoids misleading outcomes when the sequence of values of ΔY involves terms with different signs. One can use σ to evaluate the effect of nonlinear coupling between parameters. For instance, if $\sigma_{i,j} \ll \mu_{i,j}$ then the influence of the ith factor on the jth output is essentially linear and independent of the other factors. On the other hand, if $\sigma_{i,j} \gtrsim \mu_{i,j}$, then the influence is either nonlinear, or strongly coupled to other factors, or both.

An efficient strategy for sampling elementary effects is essential to the Morris method. The recommended sampling strategy is simple, and is based on the concept of a "Morris trajectory." A Morris trajectory begins at a randomly selected point on the lattice. Each step of the trajectory then consists of an elementary effect evaluation in the form of equation (2), and there is one such evaluation for each factor. The order in which the factors are taken is, however, randomly selected, and the updated value of $\mathbf{X}$ is used for the next step. So a Morris trajectory is a restricted random walk within the unit hypercube. If there are N factors, then a Morris trajectory will involve $N+1$ model

evaluations, one at the starting point and one for each subsequent step. Of course, one needs a number of Morris trajectories to adequately characterise the elementary effects, but ten or twenty is claimed to be sufficient [34, 11]. The important point is that the computational cost is linear in the number of factors.

In the present work, we have chosen to use ten lattice points on each axis, so that each factor takes one of the values $0.05, 0.15, \ldots, 0.95$, following the prescription of Campolongo et al. [11]. These discrete values are mapped to the relevant rate constants by inverting the corresponding cumulative probability distributions. This procedure means that regions of high probability density are visited more frequently than those of low density, as should be the case. Also following Campolongo et al. [11], we take $\Delta = 0.5$. With this choice, there is only one possible direction of movement at each step of the Morris trajectory, within the constraint of remaining within the unit hypercube, so that the only random elements remaining are the starting point, and the sequence of factors.

3.2. Screening Results

In this section we discuss the results of applying the Morris screening procedure described in section 3 to the reduced chemistry model presented in section 2. Twenty Morris trajectories were created for each operating point, entailing about a thousand solutions of the model for each case of interest. For each power and gas mixture, screening was carried out at $t = 3$ ms and at $t = 6$ ms, corresponding to the end of the powered segment of the model, and to the end of the simulation respectively. In general, we find that $|\mu| \approx \mu^*$, and $\sigma \sim |\mu|$. As explained above, the outcome of the Morris screening is a "ranking" of the factors that influence the uncertainty in the model outputs. In this case, the "factors" are the rate constants, and the "outputs" are the chemical species densities at the indicated time. The Morris screening, of course, only provides information about which factors are influential. It does not directly offer any insight into how this influence is exerted. Often, the mechanism of this influence is obvious, for example because the most important factors influencing a species density are the rate constants of reactions that directly produce or consume that species. Sometimes, however, influence is exerted by less direct mechanisms. For example, the recombination reaction,

$$\mathrm{He} + \mathrm{O}^- + \mathrm{O}_2^+ \rightarrow \mathrm{He} + \mathrm{O} + \mathrm{O}_2, \tag{5}$$

appears rather frequently in lists of influential factors because this reaction strongly affects the electron density, the electron density affects the density of almost every other species, and the rate constant is not specially well-known. Similarly, the rate of elastic collisions between electrons and helium shows as an influential factor when the oxygen density is low, even though this reaction evidently has no direct effect on any species density. It can, however, divert significant amounts of power into gas heating, and this exerts an indirect influence on the electron density. For these sorts of reasons, comparing the outcome of the Morris analysis with a ranking of dominant reactions directly

affecting a species density can be of interest, and we present such data in figures 6, 7 and 8. These data also emphasize that identifying dominant reaction pathways and sensitivity analysis by the Morris method offer complementary but essentially different information about the chemical system. One can, of course, guess that a reaction that is a predominant source or sink for a particular species is also likely to feature in the sensitivity ranking, and *vice versa*, but one would only be guessing, in particular because, as we have already shown [49], the uncertainty can vary in surprising ways.

Figure 6 compares the dominant reaction pathways [26, 29] and the sensitivity ranking for atomic oxygen. In this case, the dominant pathways and the most influential factors generally involve a similar group of processes, with some exceptions, such as reaction 5 above, which appears as a factor but not as an important pathway, even though is evidently does directly affect the atomic oxygen density. Of course, this is not a very well-known rate constant, and this reaction does affect the charged particle density as well. Figure 7 shows that there is a stronger correlation between dominant pathways and dominant factors in the case of $O_2(a^1\Delta_u)$, and the dominant influences here are a mixture of electron impact processes and three body recombination reactions. The quenching process

$$\mathrm{He} + \mathrm{O} + \mathrm{O}_2(a^1\Delta_u) \rightarrow \mathrm{He} + \mathrm{O} + \mathrm{O}_2, \tag{6}$$

has a particularly poorly known rate [5, 10]. A similar picture emerges for ozone, figure 8, where again one finds a mixture of three body and electron impact processes. The data shown in figures 6 to 8 refer to a single operating point, but naturally the dominant factors change in a complex way as the physical conditions change. For instance, important sinks for atomic oxygen in general are the three body processes:

$$\mathrm{He} + \mathrm{O} + \mathrm{O} \ \rightarrow \text{products} \tag{7}$$

$$\mathrm{He} + \mathrm{O} + \mathrm{O}_2 \rightarrow \mathrm{He} + \mathrm{O}_3. \tag{8}$$

The first of these reactions has a much larger rate than the second, which results in atomic oxygen recombining predominantly into diatomic states of molecular oxygen under oxygen-poor conditions. Conversely, under oxygen-rich conditions, the second reaction dominates and abundant ozone is formed. The interplay between these channels is one reason why the neutral radical composition is a strong function of the feedstock oxygen density. For reasons of this kind, a summary of the voluminous results of the Morris screening is helpful. There are of course many ways to this end, but a helpful approach is to investigate those reactions that make a contribution above a certain threshold to the uncertainty in the densities of the three species of central interest. For instance, one can search for the set of reactions that contribute more than 10 % of the total uncertainty to one or more of these three species, at any of the points where a Morris analysis has been conducted. The results of this investigation are summarized in table 3. This data shows that only nine reactions contribute to the uncertainty at this threshold. Three of these are electron impact processes, and five are three body processes involving helium. Alternative criteria lead to similar but not identical lists of

critical reactions. For instance, selecting those reactions that rank one or two in their contributions to at least one of the three species uncertainties, or that are in the group of reactions that contribute 50 % of the uncertainty to a given species, both produce almost identical lists of critical reactions. For these comparative purpose, we characterised the uncertainty by μ^*, to avoid ambiguity caused by variations in sign. In this context, less important than the exact catalogue of influential reactions is the conclusion that of the almost four hundred reactions that feature in the comprehensive model, about ten are responsible for perhaps half of the uncertainty in the model predictions. The remaining uncertainty is rather broadly distributed across the rest of the reaction scheme. For example, the set of reactions that captures 95 % of the uncertainty has forty two members, and thus includes about 80 % of the reactions in the reduced model, or about 10 % of those in the comprehensive model.

4. Discussion

The purpose of a screening exercise such as the one described in the previous section is to identify opportunities for improving the model under investigation. Clearly, the outcome—that a relatively small number of reactions have a disproportionate influence on the precision of the model predictions—immediately suggests that indeed one can appreciably improve the model by focussing attention on these sensitive coefficients. As we have already noted, there are two major groups of sensitive coefficients, namely electron impact processes involving the oxygen molecule and three body processes involving helium. These present different challenges.

The present work embarks from the comprehensive model developed previously. In that model, an uncertainty coefficient was associated with each reaction rate by reference to the primary source of the rate data. Electron impact processes were treated in the same way as every other coefficient, in this respect. However, at least some electron impact processes have undergone further handling, because they have been part of a process of fitting to transport data derived primarily from swarm experiments [37]. This is certainly the case for processes involving the the oxygen molecule[25]. The process of fitting a set of cross sections to a set of swarm coefficients is complex, but should take note of the experimental errors in the transport coefficients and in the cross sections. There is no generally accepted, systematic, approach to solving this problem, and indeed the steps actually followed are usually not fully documented, presumably because most authors feel that interest attaches to the final quality of fit, and the cross sections that achieve this result, and not to the details of how the result was arrived at. The outcome of such a process is not known to be unique, so that there is some indeterminacy in the final cross section set, but unfortunately this has rarely if ever been quantified. This indeterminacy might well be less than the error associated with measurement of individual cross sections, however. Therefore, further investigation of the fitting process might show that the uncertainty assigned to electron impact processes in the present work is too conservative, and could be reduced. This is speculation, because we have

insufficient knowledge on the uncertainties associated with fitting cross section data to transport coefficients. Further work here would be most desirable.

The second major group of processes are three body reactions involving helium. An ideal response to the identification of these processes as critical would of course be fresh measurements of the rate constants. However, the short term prospects in this respect are not good. Insofar as the present rate constants are based directly on experimental data, the original measurements were made in some cases as long ago as the nineteen-sixties, and have not been improved since [20]. Probably, designing experiments that would give clearly improved values for these rates would not be a trivial matter [5]. However, the very existence of regions of the parameter space where certain of the model predictions are highly sensitive to particular rate constants suggest an opportunity for tuning these constants as part of an experimental validation campaign. Tuning model parameters is a legitimate route to model refinement. Of course, such an exercise should take account of the initial uncertainty in the rate constants, and the uncertainty in experimental measurements, and attempt to reach an improved value for the rate constants consistent with these constraints.

That the opportunity for such tuning exists is affirmed in figure 9, which compares the uncertainty in the ozone density calculated using the reduced model described in this paper, with results from the same model when the uncertainty associated with the critical reactions listed in table 3 is excluded. These data confirm that the uncertainty is indeed almost entirely due to these critical reactions, as the Morris analysis suggests. The uncertainty that remains, however, is widely distributed across the reaction scheme, and will be difficult to dissipate.

There are good reasons for desiring an improved model for helium-oxygen plasmas. At present, many different atmospheric plasma sources are in use for biomedical applications. These vary greatly in geometrical configuration and method of plasma production, but for reasons already discussed, there is probably much less variation in the plasma conditions that are produced. This means that the constraints under which the present model has been developed probably apply to most, if not all, of these devices. Consequently, a model validated, or tuned, for one source is likely to be valid for all. This is fortunate, because it appears quite unlikely that the considerable resources needed to undertake an experimental model validation will be forthcoming for more than a small subset of the sources that have been proposed. Moreover, the kind of equipment needed to make validation measurements is both expensive and cumbersome, so that *in situ* measurements during biological experiments are unlikely. A properly validated model would therefore be an important asset in advancing the field of biomedical applications of plasmas. There are chemistries other than the helium-oxygen system to which these argument also apply, of course.

5. Conclusions

In the opening section of this paper, we noted that the typical chemistry models employed by low-temperature plasma physicists are much more complex than those found in some cognate fields. One of the aims of the present paper was to investigate whether the complexity of these models is necessary. Under the circumstances that we studied, the answer is clearly that much of the complexity is not necessary. We found that we could reduce the helium-oxygen chemistry model that we studied from a system of almost four hundred reactions to barely more than fifty, without any perceptible change in the predictions of the model. This was possible in part because we began by defining the objectives of the modelling exercise rather more tightly than is usual. But this is only apparently a compromise. Probably no one in fact expects that their model will have universal validity, or begins a modelling study without identifying the conditions of interest and the species densities of primary concern. So we have done nothing more here than make explicit what is usually implicit.

In the second part of this study, we investigated which of the rate constants within the reduced model are primarily responsible for the parametric uncertainty in the model predictions. This was done by applying a systematic screening procedure, namely the Morris method. We showed that an even smaller subset of rate constants is disproportionately influential. Hence we conclude that from the original group of some four hundred rate constants, critical attention applied to a group of about ten coefficients could effect a large improvement in the predictive efficacy of the model. This, of course, is a vastly more tractable problem than confronting the original group of four hundred coefficients.

In this paper, we have treated only a single chemistry model. If the results obtained should prove typical for plasma chemistry models, then there seems to be an opportunity for substantial improvements to be made in the practice of plasma chemistry modelling.

Acknowledgments

This work was supported by Science Foundation Ireland under grant number 08/SRC/I1411, and by COST Action MP1101 “Biomedical Applications of Atmospheric Pressure Plasmas.”

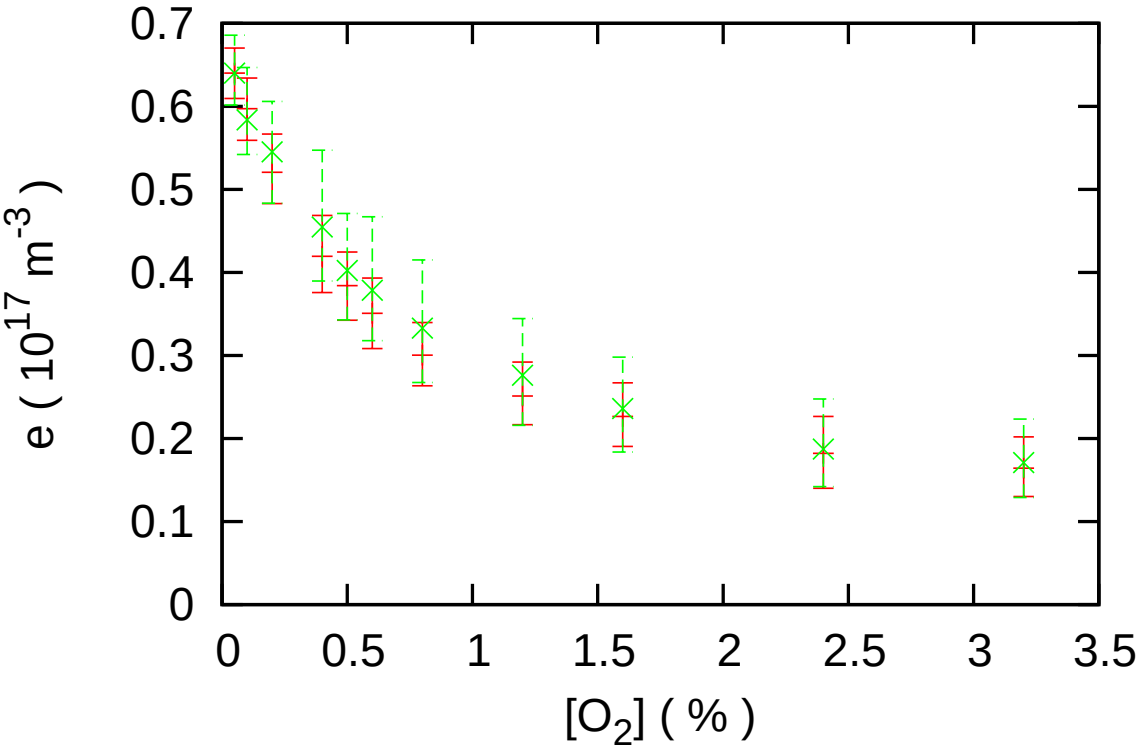

Figure 1. The electron density calculated using the comprehensive model (red) and the reduced model (green), for a constant power of 1 W, with the data sampled at the end of the power-on period, *i.e.* at 3 ms. .

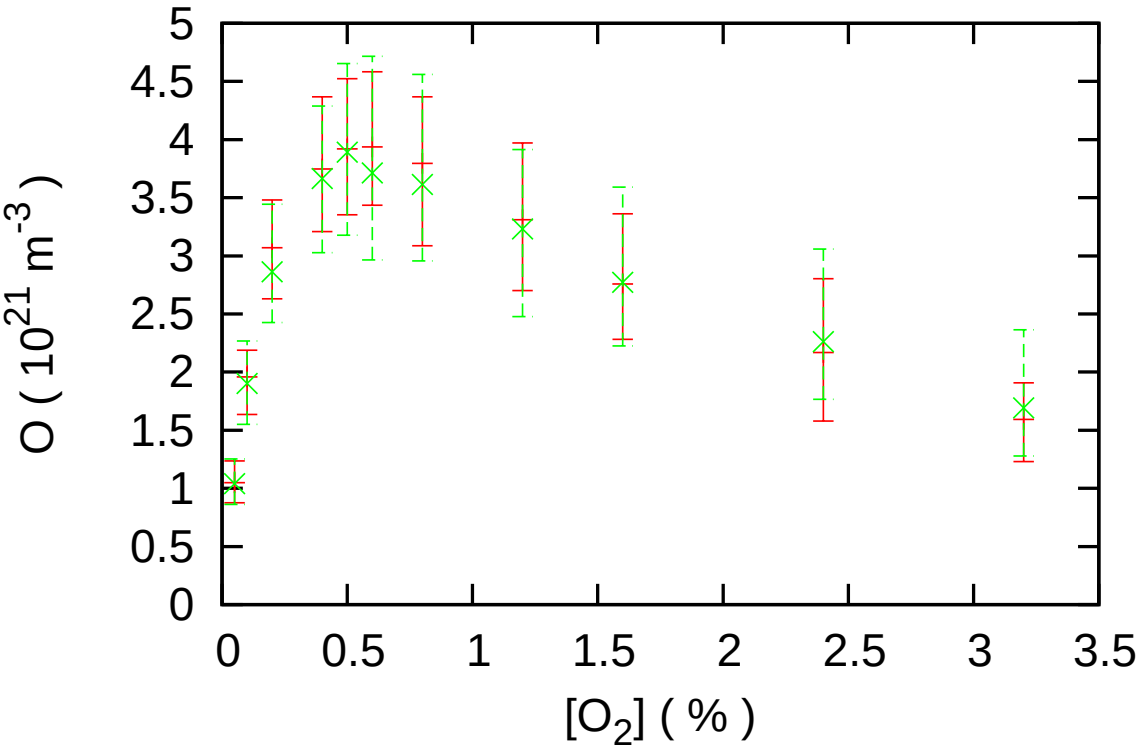

Figure 2. The density of atomic oxygen calculated using the comprehensive model (red) and the reduced model (green), for the same conditions as figure 1 .

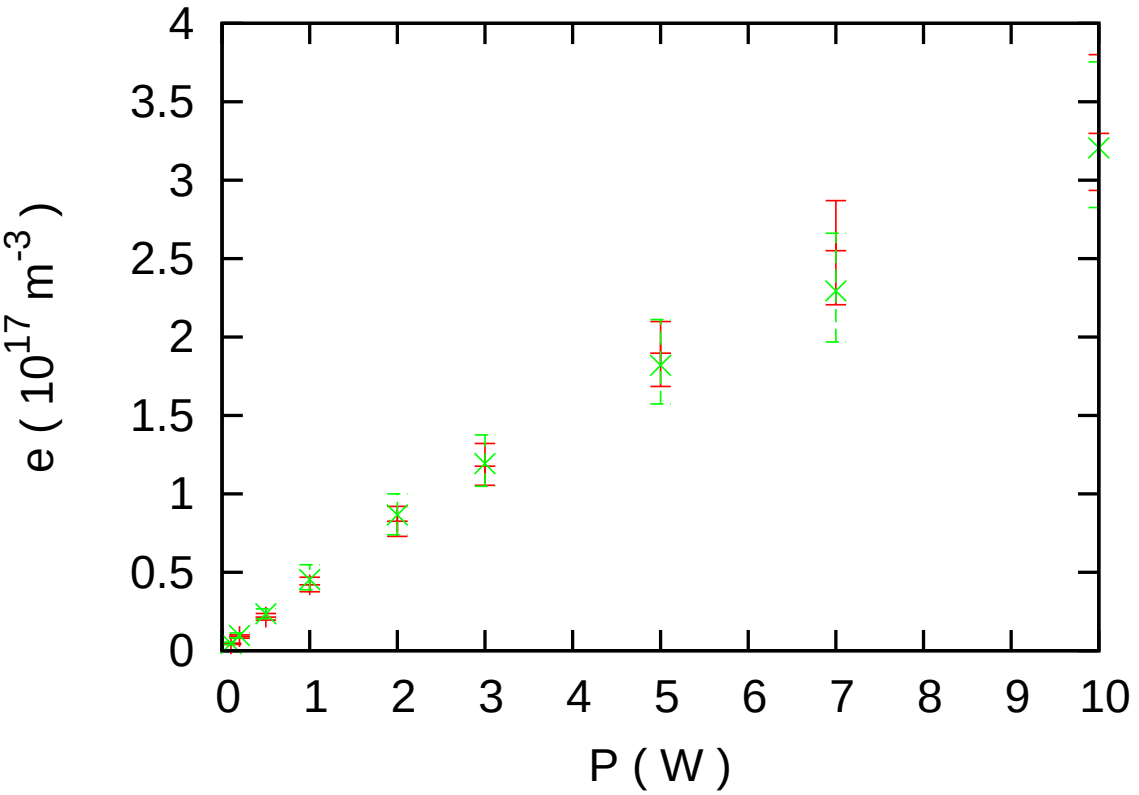

Figure 3. The electron density calculated using the comprehensive model (red) and the reduced model (green), for a constant oxygen density corresponding to $[O_2]/[He] = 0.4$ %, with the data sampled at the end of the power-on period, *i.e.* at 3 ms. .

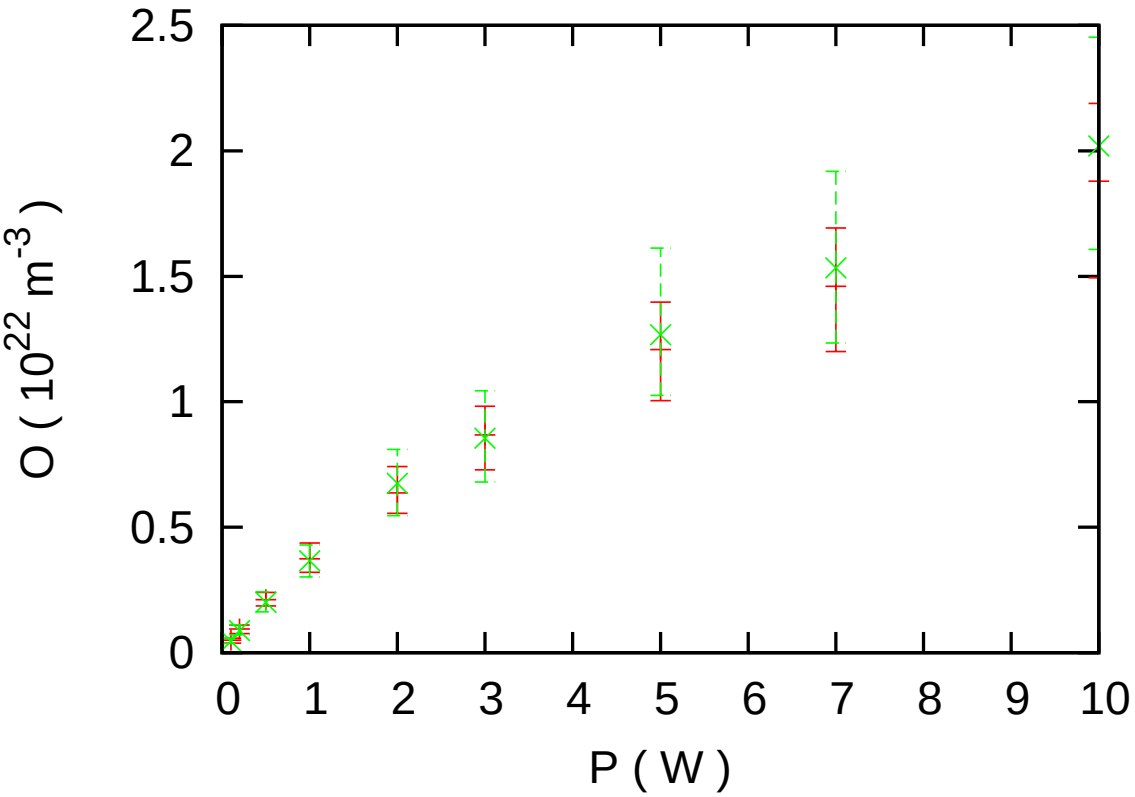

Figure 4. The atomic oxygen density calculated using the comprehensive model (red) and the reduced model (green), for the same conditions as figure 3 .

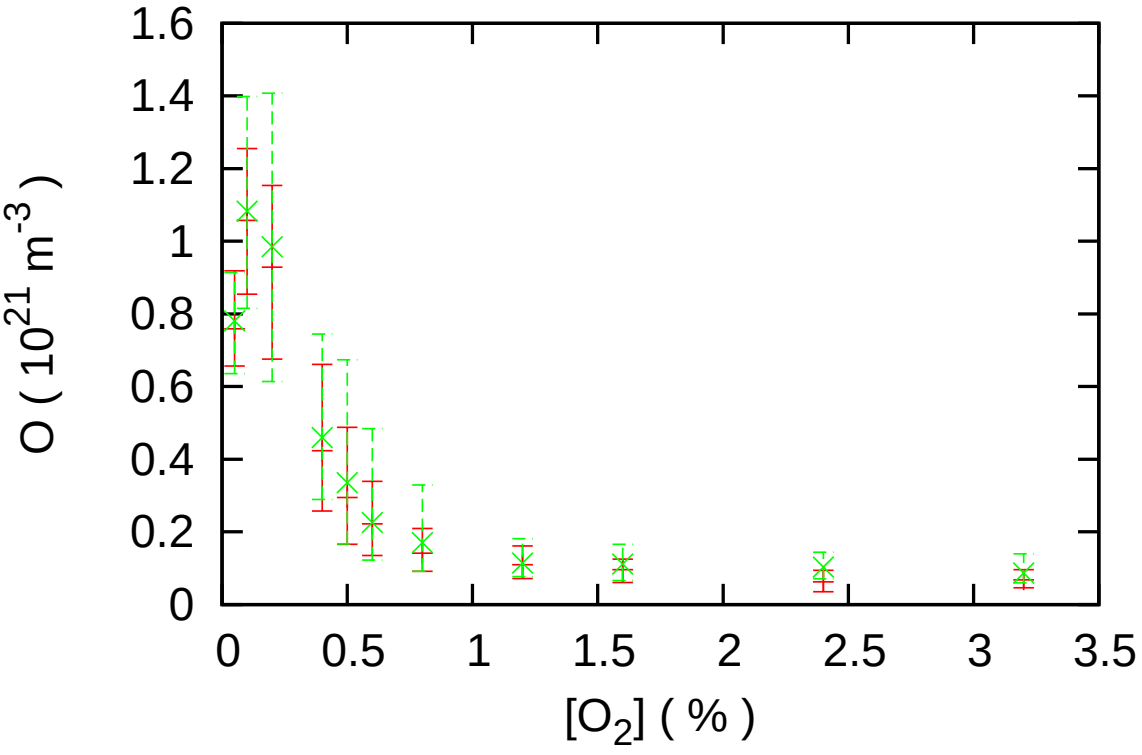

Figure 5. The atomic oxygen density calculated using the comprehensive model (red) and the reduced model (green), for a constant power of 1 W, with the data sampled at the end of the afterglow period, *i.e.* at 6 ms. .

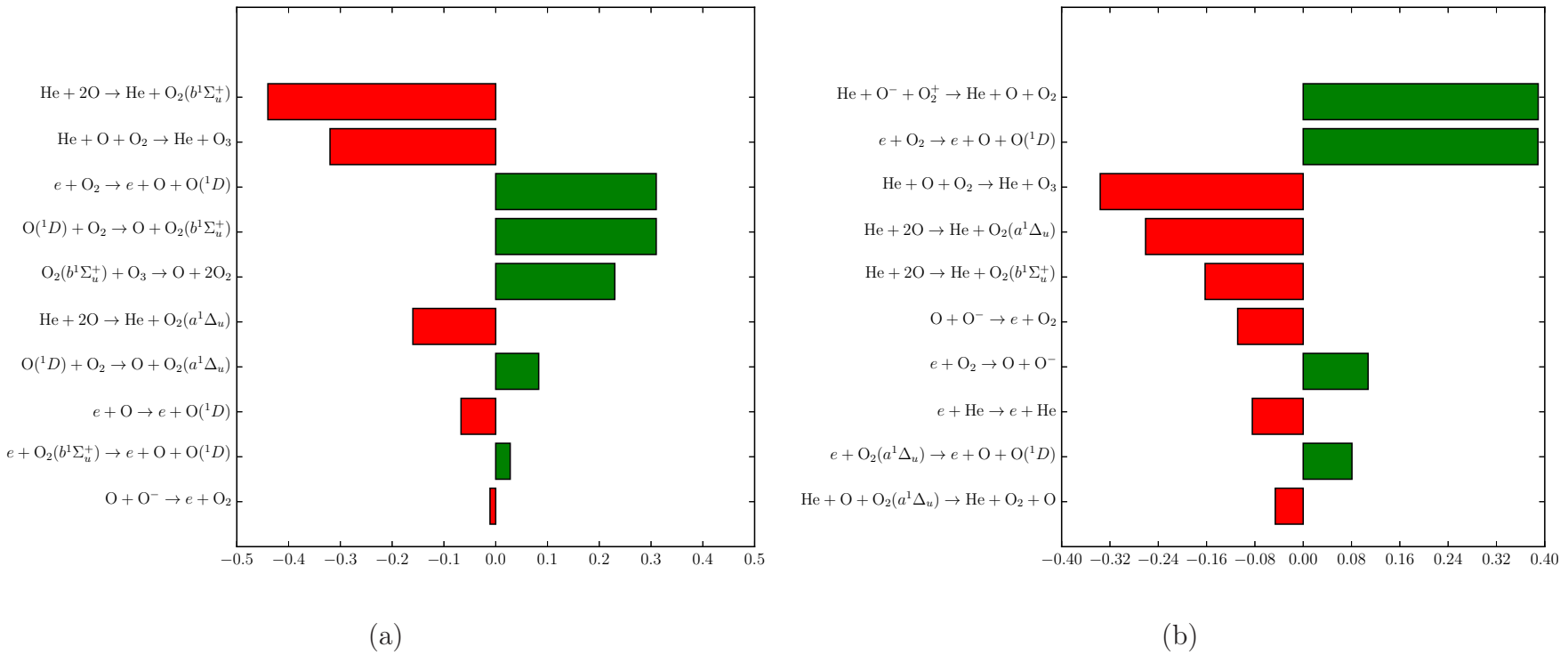

Figure 6. The left panel (a) shows the dominant reactions producing and consuming atomic oxygen during the first 3 ms of the simulation, when the plasma power is on. The right panel (b) shows the contribution to the uncertainty in the atomic oxygen density during the same interval, evaluated by the Morris method, as described in the text. The quantity shown is μ normalized by the mean density of atomic oxygen. These data were produced for a power of 1 W and a gas mixture such that $[O_2]/[He] = 0.4$ %.

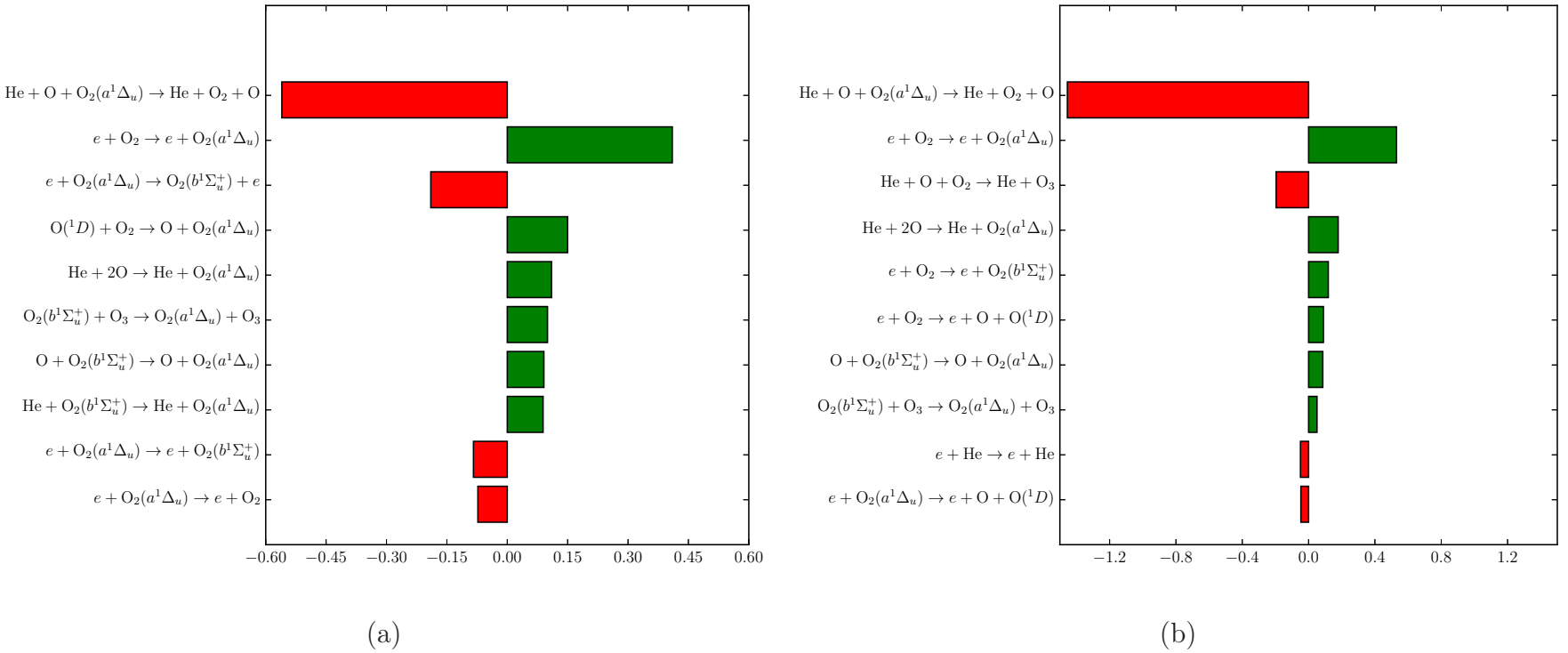

Figure 7. Dominant reactions producing and consuming $O_2(a^1\Delta_u)$, in the left panel, (a), and dominant contributions to the uncertainty of the density of the same species, in the right panel, (b). Conditions as in figure 6.

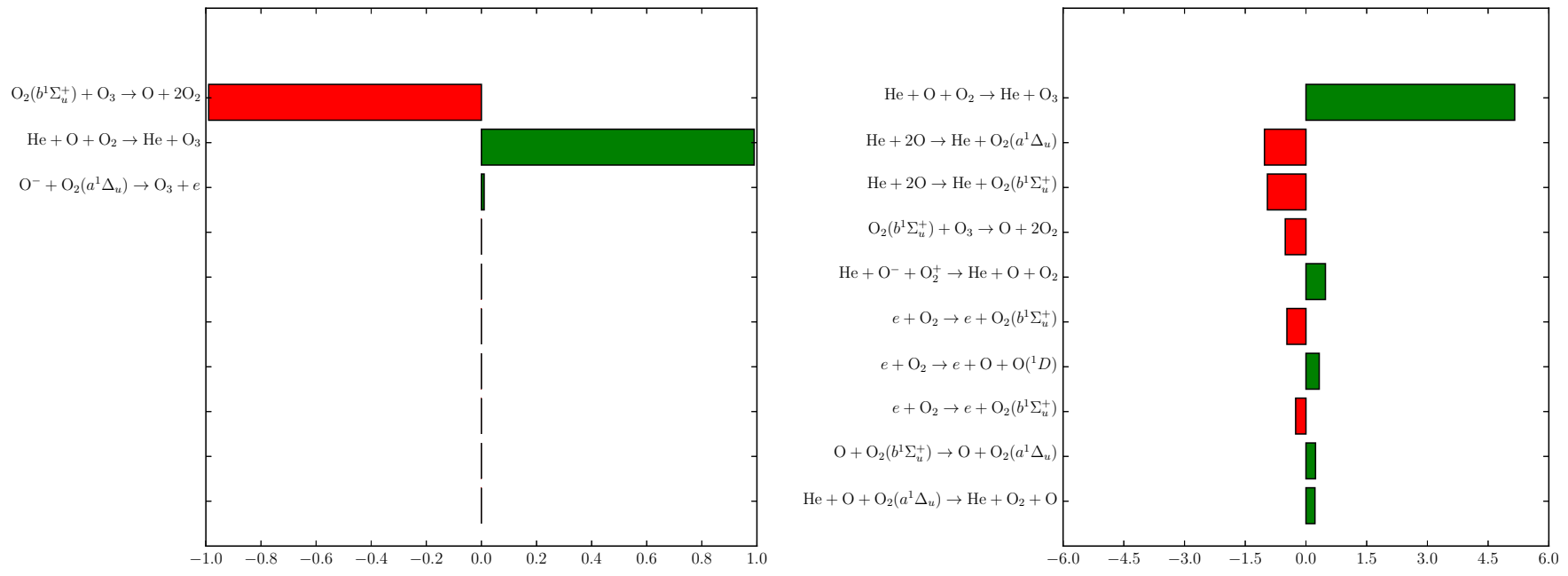

Figure 8. Dominant reactions producing and consuming ozone, in the left panel, (a), and dominant contributions to the uncertainty of the density of the same species, in the right panel, (b). Conditions as in figure 6.

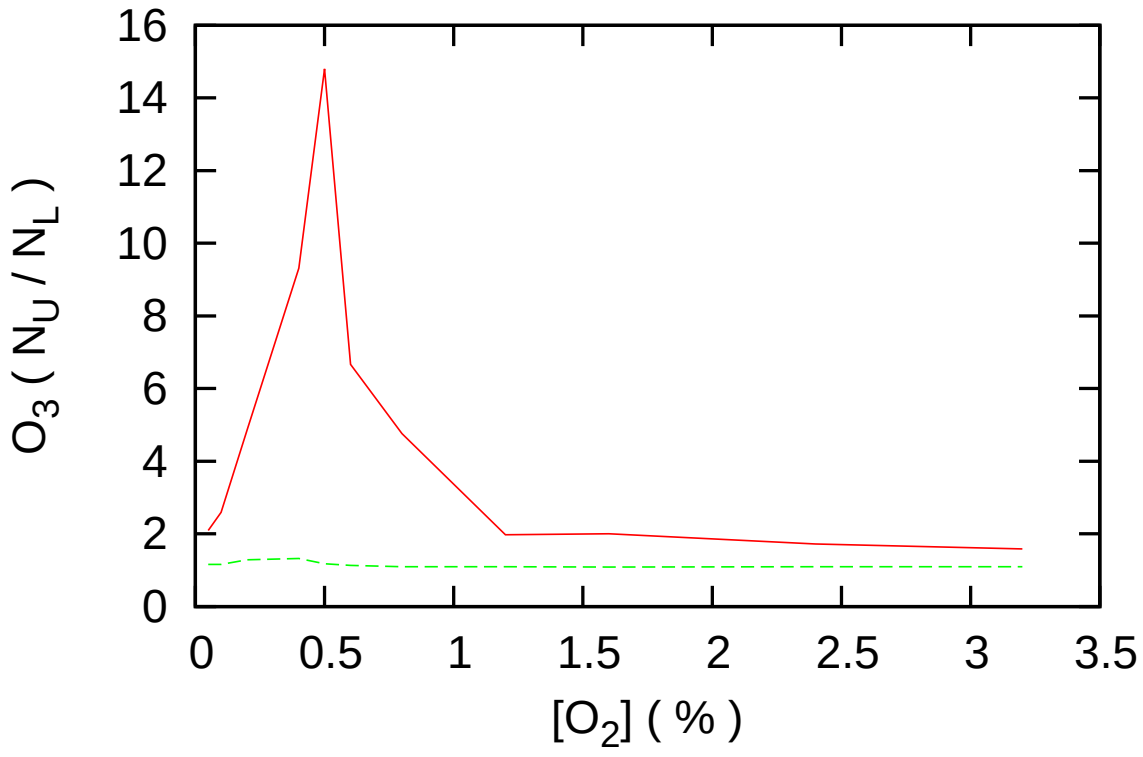

Figure 9. The uncertainty in the ozone density, for the reduced model discussed in this paper (upper curve:————), and for the same model with the uncertainty associated with the reactions in table 3 excluded (lower curve:————). This shows that, indeed, these reactions are responsible for almost all the uncertainty. N_U and N_L represent the upper and lower quartile densities from the ensemble of model predictions obtained from the Monte Carlo procedure discussed in the text. . These data are for $P = 1$ W.

Table 1: Species included in the helium-oxygen system

He
He^*
He^+
O
$O(^1D)$
O^-
O_2
$O_2(a^1\Delta_u)$
$O_2(b^1\Sigma_u^+)$
O_2^+
O_3
e

Table 2: Reactions and rate constants for the helium-oxygen system. The rubric for this table is as follows: Column 1 contains a reference number for each reaction; column 2 specifies the reaction; column 3 gives the threshold energy of the reaction, expressed in eV; column 4 gives an expression for the rate constant in MKS units, with the electron temperature expressed in eV and the neutral temperature in K; column 5 is the dimensionless uncertainty discussed in the text; and column 6 gives references.

Helium-electron chemistry						
1	$e + \mathrm{He} \rightarrow e + \mathrm{He}$	0.0	$7.77 \times 10^{-14} T_e^{0.02} \exp\left(-\frac{0.5}{T_e}\right)$	0.05	A	[1]
2	$e + \mathrm{He} \rightarrow 2e + \mathrm{He}^+$	24.6	$4.45 \times 10^{-15} T_e^{0.42} \exp\left(-\frac{26.9}{T_e}\right)$	0.05	A	[1]
3	$e + \mathrm{He} \rightarrow \mathrm{He}^* + e$	19.8	$3.3 \times 10^{-15} T_e^{0.33} \exp\left(-\frac{21.6}{T_e}\right)$	0.05	A	[1]
Oxygen-electron chemistry						
4	$e + \mathrm{O} \rightarrow e + \mathrm{O}(^1D)$	1.96	$8.45 \times 10^{-15} T_e^{-0.306} \exp\left(-\frac{3.13}{T_e}\right)$	0.3	A	[24]
5	$e + \mathrm{O}_2 \rightarrow 2e + \mathrm{O}_2^+$	12.06	$2.32 \times 10^{-15} T_e^{0.99} \exp\left(-\frac{12.51}{T_e}\right)$	0.05	A	[47, 30]
6	$e + \mathrm{O}_2 \rightarrow e + \mathrm{O} + \mathrm{O}(^1D)$	8.5	$3.12 \times 10^{-14} T_e^{0.017} \exp\left(-\frac{8.05}{T_e}\right)$	0.3	A	[25]
7	$e + \mathrm{O}_2 \rightarrow e + \mathrm{O}_2$	0.0	$4.15 \times 10^{-14} T_e^{0.599} \exp\left(-\frac{0.016}{T_e}\right)$	0.1	A	[25]
8	$e + \mathrm{O}_2 \rightarrow e + \mathrm{O}_2$	0.02	$3.88 \times 10^{-17} T_e^{-1.22} \exp\left(-\frac{0.55}{T_e}\right)$	0.3	A	[25]
9	$e + \mathrm{O}_2 \rightarrow e + \mathrm{O}_2$	0.19	$7.74 \times 10^{-16} T_e^{-1.46} \exp\left(-\frac{0.573}{T_e}\right)$	0.1	A	[25]
10	$e + \mathrm{O}_2 \rightarrow e + \mathrm{O}_2$	0.19	$2.85 \times 10^{-14} T_e^{-0.611} \exp\left(-\frac{4.72}{T_e}\right)$	0.1	A	[25]
11	$e + \mathrm{O}_2 \rightarrow e + \mathrm{O}_2(a^1\Delta_u)$	0.977	$2.1 \times 10^{-15} T_e^{-0.232} \exp\left(-\frac{2.87}{T_e}\right)$	0.3	A	[25]
12	$e + \mathrm{O}_2 \rightarrow e + \mathrm{O}_2(b^1\Sigma_u^+)$	1.627	$3.97 \times 10^{-16} T_e^{-0.089} \exp\left(-\frac{2.67}{T_e}\right)$	0.3	A	[25]
13	$e + \mathrm{O}_2 \rightarrow e + \mathrm{O}_2(b^1\Sigma_u^+)$	5.5	$2.88 \times 10^{-14} T_e^{-0.84} \exp\left(-\frac{7.07}{T_e}\right)$	0.3	A	[25]

14	$e + O_2 \rightarrow O + O^-$	0.0	$1.32 \times 10^{-15} T_e^{-1.4} \exp\left(-\frac{6.63}{T_e}\right)$	0.3	A	[25]
15	$e + O_2(a^1\Delta_u) \rightarrow e + O + O(^1D)$	8.5	$3.12 \times 10^{-14} T_e^{0.017} \exp\left(-\frac{7.07}{T_e}\right)$	0.6	C	
16	$e + O_2(a^1\Delta_u) \rightarrow e + O_2$	0.977	$2.1 \times 10^{-15} T_e^{-0.232} \exp\left(-\frac{1.89}{T_e}\right)$	0.3	A	[25]
17	$e + O_2(a^1\Delta_u) \rightarrow O_2(b^1\Sigma_u^+) + e$	0.657	$5.25 \times 10^{-15} T_e^{-0.44} \exp\left(-\frac{1.49}{T_e}\right)$	0.3	A	[48]
18	$e + O_2(a^1\Delta_u) \rightarrow e + O_2(b^1\Sigma_u^+)$	4.52	$2.88 \times 10^{-14} T_e^{-0.84} \exp\left(-\frac{6.09}{T_e}\right)$	0.3	C	
19	$e + O_2(a^1\Delta_u) \rightarrow O + O^-$	3.0	$4.14 \times 10^{-15} T_e^{-1.34} \exp\left(-\frac{5.15}{T_e}\right)$	0.3	A	[19]
20	$e + O_2(b^1\Sigma_u^+) \rightarrow e + O + O(^1D)$	8.5	$3.12 \times 10^{-14} T_e^{0.017} \exp\left(-\frac{6.42}{T_e}\right)$	0.6	C	
21	$e + O_2(b^1\Sigma_u^+) \rightarrow e + O_2(a^1\Delta_u)$	-0.657	$5.25 \times 10^{-15} T_e^{-0.44} \exp\left(-\frac{0.833}{T_e}\right)$	0.3	A	[48]
22	$e + O_2(b^1\Sigma_u^+) \rightarrow e + O_2(b^1\Sigma_u^+)$	3.87	$2.88 \times 10^{-14} T_e^{-0.84} \exp\left(-\frac{5.44}{T_e}\right)$	0.3	C	
23	$e + O_2(b^1\Sigma_u^+) \rightarrow O + O^-$	0.0	$7.11 \times 10^{-16} T_e^{-1.04} \exp\left(-\frac{0.23}{T_e}\right)$	0.5	A	[17]
24	$e + O_3 \rightarrow e + O + O_2$	2.6	$1.7 \times 10^{-14} T_e^{-0.57} \exp\left(-\frac{2.48}{T_e}\right)$	0.5	A	[16]
25	$e + O_3 \rightarrow e + O(^1D) + O_2(a^1\Delta_u)$	5.72	$3.22 \times 10^{-13} T_e^{-1.18} \exp\left(-\frac{9.17}{T_e}\right)$	0.5	A	[16]
26	$e + O_3 \rightarrow O^- + O_2$	0.0	$1.02 \times 10^{-15} T_e^{-1.3} \exp\left(-\frac{1.03}{T_e}\right)$	0.3	A	[39]
27	$e + O_3 \rightarrow O^- + O_2$	0.0	$3.45 \times 10^{-15} T_e^{-0.96} \exp\left(-\frac{1.0}{T_e}\right)$	0.3	A	[39]
Neutral chemistry of oxygen						
28	$O + O_2(b^1\Sigma_u^+) \rightarrow O + O_2(a^1\Delta_u)$	-0.65	8.0×10^{-20}	1.0	A	[42, p. 1-44][4, p. 1486]
29	$O + O_3 \rightarrow 2O_2$	0.0	$8.0 \times 10^{-18} \exp\left(-\frac{2060}{T_g}\right)$	0.2	A	[42, p. 1-35][4, p. 1475][6][50]
30	$O(^1D) + O_2 \rightarrow O + O_2(b^1\Sigma_u^+)$	0.0	$2.64 \times 10^{-17} \exp\left(\frac{55}{T_g}\right)$	0.1	A	[42, p. 1-35]
31	$O(^1D) + O_2 \rightarrow O + O_2(a^1\Delta_u)$	0.0	$6.6 \times 10^{-18} \exp\left(\frac{55}{T_g}\right)$	0.1	A	[42, p. 1-35]
32	$O(^1D) + O_3 \rightarrow 2O + O_2$	0.0	1.2×10^{-16}	0.2	A	[42, 4, 46]
33	$O(^1D) + O_3 \rightarrow 2O_2$	0.0	1.2×10^{-16}	0.2	A	[42, 4, 46]
34	$O_2 + O_2(b^1\Sigma_u^+) \rightarrow O_2 + O_2(a^1\Delta_u)$	0.0	3.8×10^{-23}	0.5	A	[42, p. 1-44][21][22]
35	$O_2(b^1\Sigma_u^+) + O_3 \rightarrow O + 2O_2$	0.0	$2.4 \times 10^{-17} \left(\frac{T_g}{300}\right)^{0.5} \exp\left(-\frac{135}{T_g}\right)$	0.2	A	[42, 4]

36	$O_2(b^1\Sigma_u^+) + O_3 \rightarrow O_2 + O_3$	0.0	$5.5 \times 10^{-18} \left(\frac{T_g}{300}\right)^{0.5} \exp\left(-\frac{135}{T_g}\right)$	0.2	A	[42, 4]
37	$O_2(b^1\Sigma_u^+) + O_3 \rightarrow O_2(a^1\Delta_u) + O_3$	0.0	$5.5 \times 10^{-18} \left(\frac{T_g}{300}\right)^{0.5} \exp\left(-\frac{135}{T_g}\right)$	0.2	A	[42, 4]
Ion chemistry of oxygen						
38	$e + 2O_2 \rightarrow O^- + O + O_2$	0.0	$1.4 \times 10^{-41} \left(\frac{300}{T_g}\right) \exp\left(-\frac{600}{T_g}\right)$	0.3	A	[7, p. 24-10]
39	$O + O^- \rightarrow e + O_2$	0.0	$2.3 \times 10^{-16} \left(\frac{300}{T_g}\right)^{1.3}$	0.4	A	[8, 3]
40	$O^- + O_2(a^1\Delta_u) \rightarrow O_3 + e$	0.0	6.1×10^{-17}	0.3	A	[31]
41	$O^- + O_3 \rightarrow e + 2O_2$	0.0	3.0×10^{-16}	0.4	A	[27][18, p. 195]
Neutral chemistry of helium-oxygen mixtures						
42	$He + 2O \rightarrow He + O_2(a^1\Delta_u)$	0.0	$2.0 \times 10^{-45} \left(\frac{300}{T_g}\right) \exp\left(-\frac{170}{T_g}\right)$	1.0	A	[20, 45]
43	$He + 2O \rightarrow He + O_2(b^1\Sigma_u^+)$	0.0	$2.0 \times 10^{-45} \left(\frac{300}{T_g}\right) \exp\left(-\frac{170}{T_g}\right)$	1.0	A	[20, 45]
44	$He + O + O_2 \rightarrow He + O_3$	0.0	$3.0 \times 10^{-46} \left(\frac{300}{T_g}\right)^{2.6}$	0.5	A	[4, 46, 12]
45	$He + O + O_2(a^1\Delta_u) \rightarrow He + O_2 + O$	0.0	4.0×10^{-45}	3.0	A	[5, 10]
46	$He + O_2(b^1\Sigma_u^+) \rightarrow He + O_2(a^1\Delta_u)$	0.0	$4.3 \times 10^{-24} \left(\frac{T_g}{300}\right)^{0.5}$	0.03	A	[21]
47	$He^* + O_2 \rightarrow e + He + O_2^+$	0.0	2.6×10^{-16}	0.2	A	[38]
Ion chemistry of helium-oxygen mixtures						
48	$e + He + O_2 \rightarrow He + O + O^-$	0.0	$1.0 \times 10^{-44} T_e^{-0.5}$	2.0	A	[13]
49	$He + O^- + O_2^+ \rightarrow He + O + O_2$	0.0	$2.0 \times 10^{-37} \left(\frac{300}{T_g}\right)^{2.5}$	3.0	B	[9]
50	$He^+ + O_2 \rightarrow He + O_2^+$	0.0	3.0×10^{-17}	0.1	A	[2][18, p. 113]

Table 3: Summary of those reactions that contribute more than 10 % to the uncertainty in any one of the three neutral species O, $O_2(a^1\Delta_u)$ and O_3. The numbers in the table indicate the maximum contribution made by each reaction to the uncertainty in the indicated species. Each datum may originate from a Morris analysis at a distinct operating condition, so, for example, there is no constraint on the results of summation along a row or column.

	O	$O_2(a^1\Delta_u)$	O_3
$e + O_2 \rightarrow e + O + O(^1D)$	0.25		0.19
$e + O_2 \rightarrow e + O_2(a^1\Delta_u)$		0.42	
$e + O_2 \rightarrow e + O_2(b^1\Sigma_u^+)$			0.17
$He + 2O \rightarrow He + O_2(a^1\Delta_u)$	0.23		0.17
$He + 2O \rightarrow He + O_2(b^1\Sigma_u^+)$	0.3		0.29
$He + O + O_2 \rightarrow He + O_3$	0.48	0.12	0.46
$He + O + O_2(a^1\Delta_u) \rightarrow He + O_2 + O$		0.56	0.19
$He + O^- + O_2^+ \rightarrow He + O + O_2$	0.22	0.12	0.25
$O_2(b^1\Sigma_u^+) + O_3 \rightarrow O + 2O_2$			0.15

References

[1] L L Alves, K Bartschat, S F Biagi, M C Bordage, L C Pitchford, C M Ferreira, G J M Hagelaar, W L Morgan, S Pancheshnyi, A V Phelps, V Puech, and O Zatsarinny. Comparisons of sets of electron–neutral scattering cross sections and swarm parameters in noble gases: II. helium and neon. *J. Phys. D: Appl. Phys.*, 46(33):334002, August 2013. ISSN 0022-3727, 1361-6463.

[2] Vincent G Anicich. Evaluated bimolecular ion-molecule gas phase kinetics of positive-ions for use in modeling planetary atmospheres, cometary comae, and interstellar clouds. *J. Phys. Chem. Ref. Data*, 22(6):1469–1569, 1993.

[3] Shaun G. Ard, Joshua J. Melko, Bin Jiang, Yongle Li, Nicholas S. Shuman, Hua Guo, and Albert A. Viggiano. Temperature dependences for the reactions of O_2^- and O^- with N and O atoms in a selected-ion flow tube instrument. *J. Chem. Phys.*, 139(14):144302, 2013. ISSN 00219606.

[4] R. Atkinson, D. L. Baulch, R. A. Cox, J. N. Crowley, R. F. Hampson, R. G. Hynes, M. E. Jenkin, M. J. Rossi, and J. Troe. Evaluated kinetic and photochemical data for atmospheric chemistry: Volume I - gas phase reactions of O_x, HO_x, NO_x and SO_x species. *Atmos. Chem. Phys.*, 4(6):1461–1738, September 2004. ISSN 1680-7324.

[5] Valeriy N. Azyazov, Paul Mikheyev, David Postell, and Michael C. Heaven.

$O_2(a^1\Delta)$ quenching in the $O/O_2/O_3$ system. *Chem. Phys. Lett.*, 482(1-3):56–61, November 2009. ISSN 00092614.

[6] D L Baulch, R A Cox, R F Hampson, Jr, J A Kerr, J Troe, and R T Watson. Evaluated kinetic and photochemical data for atmospheric chemistry: Supplement II. CODATA task group on gas phase chemical kinetics. *J. Phys. Chem. Ref. Data*, 13(4):1259–1378, 1984.

[7] Theodore Baurer and Marlyn H Bortner. Defense Nuclear Agency Reaction Rate Handbook. Second Edition. Revision Number 7. Technical Report DNA-1948H-Rev-7, General Electric Company, 1978.

[8] S. G. Belostotsky, D. J. Economou, D. V. Lopaev, and T. V. Rakhimova. Negative ion destruction by $O(^3P)$ atoms and $O_2(a^1\Delta_g)$ molecules in an oxygen plasma. *Plasma Sources Sci. Technol.*, 14(3):532, August 2005. ISSN 0963-0252.

[9] Manfred A. Biondi. Atmospheric electron-ion and ion-ion recombination processes. *Can. J. Chem.*, 47(10):1711–1719, 1969.

[10] O V Braginskiy, A N Vasilieva, K S Klopovskiy, A S Kovalev, D V Lopaev, O V Proshina, T V Rakhimova, and A T Rakhimov. Singlet oxygen generation in O_2 flow excited by RF discharge: I. homogeneous discharge mode: α-mode. *J. Phys. D: Appl. Phys.*, 38(19):3609–3625, October 2005. ISSN 0022-3727, 1361-6463.

[11] Francesca Campolongo, Jessica Cariboni, and Andrea Saltelli. An effective screening design for sensitivity analysis of large models. *Environmental Modelling & Software*, 22(10):1509–1518, October 2007. ISSN 13648152.

[12] E. Castellano and H. J. Schumacher. Die kinetik des photochemischen zerfalles von ozon in rot-gelbem licht. *Z. Phys. Chem.*, 34(1-4):198–212, September 1962. ISSN 0942-9352.

[13] L. M. Chanin, A. V. Phelps, and M. A. Biondi. Measurements of the attachment of low-energy electrons to oxygen molecules. *Phys. Rev.*, 128(1):219–230, October 1962.

[14] W. Van Gaens and A. Bogaerts. Kinetic modelling for an atmospheric pressure argon plasma jet in humid air. *J. Phys. D: Appl. Phys.*, 46(27):275201, July 2013. ISSN 0022-3727.

[15] David B. Graves. Low temperature plasma biomedicine: A tutorial review. *Phys. Plasmas 1994-Present*, 21(8):080901, August 2014. ISSN 1070-664X, 1089-7674.

[16] Monika Gupta and K. L. Baluja. Electron collisions with an ozone molecule using the R-matrix method. *J. Phys. B: At. Mol. Opt. Phys.*, 38(22):4057, November 2005. ISSN 0953-4075.

[17] Daiyu Hayashi and Kiyoshi Kadota. Efficient production of O^- by dissociative attachment of slow electrons to highly excited metastable oxygen molecules. *Jpn. J. Appl. Phys.*, 38(1R):225, January 1999. ISSN 1347-4065.

[18] Yasumasa Ikezoe. *Gas Phase Ion-molecule Reaction Rate Constants Through 1986*. Ion Reaction Research Group of the Mass Spectroscopy Society of Japan, 1987.

[19] Thomas Jaffke, Martina Meinke, Reza Hashemi, Loucas G. Christophorou, and Eugen Illenberger. Dissociative electron attachment to singlet oxygen. *Chem. Phys. Lett.*, 193(1–3):62–68, May 1992. ISSN 0009-2614.

[20] Harold S Johnston. Gas phase reaction kinetics of neutral oxygen species. Technical Report NSRDS-NBS-20, National Bureau of Standards, September 1968.

[21] Paul L. Kebabian and Andrew Freedman. Rare gas quenching of metastable O_2 at 295 K. *J. Phys. Chem. A*, 101(42):7765–7767, October 1997. ISSN 1089-5639.

[22] Mark B. Knickelbein, Kenneth L. Marsh, Otho E. Ulrich, and George E. Busch. Energy transfer kinetics of singlet molecular oxygen: The deactivation channel for $O_2(b^1\Sigma_u^+)$. *J. Chem. Phys.*, 87(4):2392, August 1987. ISSN 00219606.

[23] Kamal Kumar and Chih-Jen Sung. Autoignition of methanol: Experiments and computations. *Int. J. Chem. Kinet.*, 43(4):175–184, April 2011. ISSN 05388066.

[24] Russ R. Laher and Forrest R. Gilmore. Updated excitation and ionization cross sections for electron impact on atomic oxygen. *J. Phys. Chem. Ref. Data*, 19(1): 277–305, January 1990. ISSN 0047-2689, 1529-7845.

[25] S. A. Lawton and A. V. Phelps. Excitation of the $b^1\Sigma_g^+$ state of O_2 by low energy electrons. *J. Chem. Phys.*, 69(3):1055–1068, 1978. ISSN 0021-9606, 1089-7690.

[26] Ralph Lehmann. An algorithm for the determination of all significant pathways in chemical reaction systems. *J. Atmos. Chem.*, 47(1):45–78, January 2004. ISSN 0167-7764, 1573-0662.

[27] C. Lifshitz, R. L. C. Wu, J. C. Haartz, and T. O. Tiernan. Associative detachment reactions of negative ions with O_3. *J. Chem. Phys.*, 67(5):2381, 1977. ISSN 00219606.

[28] U. Maas and S. B. Pope. Simplifying chemical kinetics: Intrinsic low-dimensional manifolds in composition space. *Combustion and Flame*, 88(3–4):239–264, March 1992. ISSN 0010-2180.

[29] A. H. Markosyan, A. Luque, F. J. Gordillo-Vázquez, and U. Ebert. Pumpkin: A tool to find principal pathways in plasma chemical models. *Comp. Phys. Comm.*, 185(10):2697–2702, October 2014. ISSN 0010-4655.

[30] J.W. McConkey, C.P. Malone, P.V. Johnson, C. Winstead, V. McKoy, and I. Kanik. Electron impact dissociation of oxygen-containing molecules–a critical review. *Phys. Rep.*, 466(1-3):1–103, September 2008. ISSN 03701573.

[31] Anthony Midey, Itzhak Dotan, and A. A. Viggiano. Temperature dependences for the reactions of O^- and O_2^- with $O_2(a^1\Delta_g)$ from 200 to 700 K. *J. Phys. Chem. A*, 112(14):3040–3045, April 2008. ISSN 1089-5639, 1520-5215.

[32] D D Monahan and M M Turner. Global models of electronegative discharges: critical evaluation and practical recommendations. *Plasma Sources Sci. Technol.*, 17(4):045003, November 2008. ISSN 0963-0252, 1361-6595.

[33] Derek D. Monahan and Miles M. Turner. On the global model approximation. *Plasma Sources Sci. Technol.*, 18(4):045024, 2009. ISSN 0963-0252.

[34] Max D. Morris. Factorial sampling plans for preliminary computational experiments. *Technometrics*, 33(2):161–174, 1991.

[35] Sebastian Mosbach, Je Hyeong Hong, George P. E. Brownbridge, Markus Kraft, Soumya Gudiyella, and Kenneth Brezinsky. Bayesian error propagation for a kinetic model of n-propylbenzene oxidation in a shock tube. *Int. J. Chem. Kinet.*, 46(7): 389–404, July 2014. ISSN 1097-4601.

[36] Tomoyuki Murakami, Kari Niemi, Timo Gans, Deborah O'Connell, and William G. Graham. Chemical kinetics and reactive species in atmospheric pressure helium–oxygen plasmas with humid-air impurities. *Plasma Sources Sci. Technol.*, 22(1):015003, February 2013. ISSN 0963-0252.

[37] Z Lj Petrović, S Dujko, D Marić, G Malović, ž Nikitović, O Šašić, J Jovanović, V Stojanović, and M Radmilović-Rađenović. Measurement and interpretation of swarm parameters and their application in plasma modelling. *Journal of Physics D: Applied Physics*, 42(19):194002, October 2009. ISSN 0022-3727, 1361-6463.

[38] J. M. Pouvesle, A. Khacef, J. Stevefelt, H. Jahani, V. T. Gylys, and C. B. Collins. Study of two-body and three-body channels for the reaction of metastable helium atoms with selected atomic and molecular species. *Journal of Chemical Physics*, 88(5):3061, 1988. ISSN 00219606.

[39] S. A. Rangwala, S. V. K. Kumar, E. Krishnakumar, and N. J. Mason. Cross sections for the dissociative electron attachment to ozone. *J. Phys. B: At. Mol. Opt. Phys.*, 32(15):3795, August 1999. ISSN 0953-4075.

[40] Yukinori Sakiyama, David B Graves, Hung-Wen Chang, Tetsuji Shimizu, and Gregor E Morfill. Plasma chemistry model of surface microdischarge in humid air and dynamics of reactive neutral species. *J. Phys. D: Appl. Phys.*, 45(42): 425201, October 2012. ISSN 0022-3727, 1361-6463.

[41] Andrea Saltelli, Marco Ratto, Stefano Tarantola, and Francesca Campolongo. Sensitivity analysis for chemical models. *Chem. Rev.*, 105(7):2811–2828, July 2005. ISSN 0009-2665, 1520-6890.

[42] S P Sander, R R Freidl, J R Barker, D M Golden, M J Kurylo, P H Wine, J P D Abbatt, J B Burkholder, C E Kolb, G K Moortgat, R E Huie, and V L Orkin. Chemical kinetics and photochemical data for use in atmospheric studies. Technical Report JPL Publication 10-6, Jet Propulsion Laboratory, June 2011.

[43] V. Schulz-von der Gathen, V. Buck, T. Gans, N. Knake, K. Niemi, St. Reuter, L. Schaper, and J. Winter. Optical diagnostics of micro discharge jets. *Contr. Plasma Phys.*, 47(7):510–519, November 2007. ISSN 08631042, 15213986.

[44] Rex T. Skodje, Alison S. Tomlin, Stephen J. Klippenstein, Lawrence B. Harding, and Michael J. Davis. Theoretical validation of chemical kinetic mechanisms: Combustion of methanol. *J. Phys. Chem. A*, 114(32):8286–8301, August 2010. ISSN 1089-5639, 1520-5215.

[45] Tom G. Slanger and Richard A. Copeland. Energetic oxygen in the upper atmosphere and the laboratory. *Chem. Rev.*, 103(12):4731–4766, 2003.

[46] Jeffrey I. Steinfeld, Steven M. Adler-Golden, and Jean W. Gallagher. Critical survey of data on the spectroscopy and kinetics of ozone in the mesosphere and thermosphere. *J. Phys. Chem. Ref. Data*, 16(4):911–951, October 1987. ISSN 0047-2689, 1529-7845.

[47] H. C. Straub, P. Renault, B. G. Lindsay, K. A. Smith, and R. F. Stebbings. Absolute partial cross sections for electron-impact ionization of H_2, N_2, and O_2 from threshold to 1000 eV. *Phys. Rev. A*, 54(3):2146–2153, September 1996.

[48] Motomichi Tashiro, Keiji Morokuma, and Jonathan Tennyson. R-matrix calculation of electron collisions with electronically excited O_2 molecules. *Phys. Rev. A*, 73(5):052707, May 2006.

[49] Miles M Turner. Uncertainty and error in complex plasma chemistry models. *Plasma Sources Science and Technology*, 24(3):035027, June 2015. ISSN 0963-0252, 1361-6595.

[50] P. H. Wine, J. M. Nicovich, R. J. Thompson, and A. R. Ravishankara. Kinetics of $O(^3P_j)$ reactions with hydrogen peroxide and ozone. *J. Phys. Chem.*, 87(20): 3948–3954, September 1983. ISSN 0022-3654.

[51] Judit Zádor, István Gy. Zsély, Tamás Turányi, Marco Ratto, Stefano Tarantola, and Andrea Saltelli. Local and global uncertainty analyses of a methane flame model. *J. Phys. Chem. A*, 109(43):9795–9807, November 2005. ISSN 1089-5639, 1520-5215.